Heliyon 10 (2024) e39021

Contents lists available at ScienceDirect

Heliyon

journal homepage: www.cell.com/heliyon

Research article

Establishment of RNA modification regulators index predicting clinical outcomes and immune relevance of kidney cancer patients

Gang Li [a,1], Jingmin Cui [a,1], Shuang He [b,1], Xiufang Feng [a], Wenhan Li [a], Tao Li [a], Peilin Chen [a,*]

[a] Department of Urology, Tangshan Gongren Hospital, 27 Wenhua Road, Tangshan, 063000, Hebei, China
[b] Tangshan Lunan District First Nursery Center (Lunan District First Kindergarten), China

ARTICLE INFO

Keywords:
RNA modifcation
RNA regulators
Risk model
Immune therapy
RCC

ABSTRACT

Increasing evidence indicates that RNA modifications are misregulated in human cancers, which might be optimal targets of cancer therapy. However, important RNA regulators in kidney cancer still need further exploration. In this study, we collected regulators representing different types of RNA modification and identified the prognosis-related RNA regulators in kidney cancer patients. We further constructed a 4-gene RNA regulators signature and index called prognosis-related RNA regulators index (PRRI) by the Lasso-Cox regression algorithm. We found that PRRI could precisely predict prognosis of patients in the KIRC training (AUC at 3-/5-/7-years = 0.7132/0.7220/0.7283) and testing cohorts (AUC at 3-/5-/7-years = 0.7141/0.7403/0.7305) and two independent RCC cohorts - E-MTAB-1980 (AUC at 3-/5-/7-years = 0.7036/0.7385/0.7143) and KIRP (AUC at 3-/5-/7-years = 0.6203/0.6365/0.6941). Moreover, the high PRRI group showed a worse clinical outcome than the low PRRI group. PRRI demonstrated strong robustness and was related to histological grade and pathologic stage, which was also found to be an independent prognosis factor when other clinical variables adjusted it. We further found several immune-related pathways differentially enriched in the high or low PRRI group. The regulation of T cell migration, which has been proven to be an immunosuppressive cell, shows a high enrichment in the high PRRI group. Further analysis reveals that PRRI also shows a highly positive correlation with the activity of Tregs. TIDE analysis and two independent immune therapy cohorts revealed that the high PRRI group might resist immune therapy, while the low PRRI group might benefit from the treatment, indicating that PRRI could be a marker for predicting immune therapeutic response. All in all, we determined 4 potentially essential RNA regulators and illustrated their mechanisms concretely. Furthermore, we constructed a 4-gene index called PRRI to predict patients' outcomes and immunotherapy response.

1. Introduction

Various types of RNA have been found to exist in the human transcriptome, and each of them plays its own vital role in guaranteeing the physical function of cells [1–3]. RNA could be modified to participate in the post-transcriptional regulation of gene

* Corresponding author.
E-mail address: peilinchen5566@126.com (P. Chen).
[1] Gang Li, Jingmin Cui, Shuang He contribute equal to this article.

https://doi.org/10.1016/j.heliyon.2024.e39021
Received 29 June 2024; Received in revised form 27 September 2024; Accepted 4 October 2024
Available online 5 October 2024

expression. So far, over 170 types of RNA modifications have been found to regulate not only RNA but non-coding RNA as well [4,5]. RNA modifications generally influence RNA stability, localization, RNA-RNA interaction, RNA-protein interaction, and RNA splicing, etc. Specific regulators could regulate different types of RNA modification. The abnormalities and alterations of these regulators in modulating RNA modification patterns are related to the emergence of various diseases, such as cancer [6].

Previous studies have reported that RNA modification abnormalities could affect biological behaviors of multiple cancers, such as cell proliferation, differentiation, stemness, metabolism, migration, and therapeutic resistance [7–11]. Among these, N6-methyladenosine (m^6A), 5-methylcytidine (m^5C), and N7-methylguanosine (m^7G) modification are found to be closely correlated with tumorigenesis and progression of cancer [12]. m6A is the most prevalent RNA modification on eukaryotic mRNA. The alteration of m^6A levels participates in cancer pathogenesis and development via regulating several genes' expression, such as *BRD4*, *MYC*, *SOCS2*, and *EGFR*, which have been proven to play an important role in cancer [9]. m^5C is a crucial post-transcriptional modification on mammalian mRNA, which has been reported to be involved in the development of cancer and correlated with multiple cancer-related pathways [13,14]. m^1A in tRNA is dramatically elevated and correlated with cancer stemness and patients' poor prognosis in liver cancer [15]. Though many studies show the essential roles of RNA modification in cancers, the effects of them on many aspects of malignant behavior remain unknown. For example, little attention has been paid to inspecting the relation and mechanisms of m^5C modification in tumor drug resistance [10]. In kidney cancer, m^6A-modified *TRAF1* regulated by *METTL13*, a m^6A writer, could promote sunitinib resistance by influencing apoptosis and angiogenesis [16]. *FTO*, a m^6A eraser (demethylase), whose aberrant activation could render *HIF2*$\alpha^{low/-}$ clear cell renal cell carcinoma sensitive to *BRD9* inhibitors [17]. m^6A reader, *YTHDC1*, also has been found to be regulated by the *YY1/HDAC2* complex, modulating the progression and chemosensitivity of kidney cancer [18].

Some research has revealed the potential role of m6A regulators in kidney cancer. However, the functions of other types of RNA modification, as well as their own regulators on regulating kidney cancer, still remain unclear. For example, m^5C modification, which had been reported to play an important role in bladder cancer, represents no studies about the concrete mechanisms in kidney cancer, even though there are some studies reveal the potential functions of m^5C regulators in kidney cancer by bioinformatics methods [19, 20]. Cumulative evidence has revealed the role of RNA modification in cancer, and more and more research has been carried out exploring the mechanisms, so it is necessary to exploit the potential important RNA modification regulators for further pre-clinical research in kidney cancer.

In our study, we obtained RNA regulators and determined prognosis-related RNA regulators in the KIRC cohort. We explicitly illustrate the expression alteration and mechanisms of these genes by multiple bioinformatics methods. Based on the machine learning algorithm, we constructed a four-gene index called PRRI to predict clinical outcomes and immune therapeutic responses of cancer patients. These findings might provide a theoretical foundation for further pre-clinical and clinical research.

2. Material and methods

2.1. Collection of data

The RNA regulators were obtained from the summarized table list of previous research, all commonly known RNA regulators representing different RNA modification methods (including ac4C, I, M1A, M5C, M6A, M7G, ψ, cm5U, mcm5 s2 U/cm5U) from previous research were included in this study [21] (Table S1). Then, we collected the transcriptome of KIRC and KIRP (FPKM units) (version: 07-19-2019) from the public website UCSC Xena (**http://xena.ucsc.edu/**) [22]. The KIRC dataset contains 535 tumors and 72 normal samples, and the KIRP dataset contains 285 tumor samples. We transformed the expression format of KIRC and KIRP cohorts into TPM units according to the public method (**https://haroldpimentel.wordpress.com/2014/05/08/what-the-fpkm-a-review-rna-seq-expression-units/**) so that we could analyze them. In addition, we downloaded the processed normalized expression data of the E-MTAB-1980 **(Release Date: October 16, 2013)** from the Array Express database (https://www.ebi.ac.uk/arrayexpress), whose corresponding clinical data was obtained from the published literature [23]. E-MTAB-1980 mRNA dataset contains 101 RCC tumor tissue. The clinical data of KIRC, KIRP, and E-MTAB-1980 were also downloaded from their corresponding website; the samples that have corresponding mRNA expression data were included in this study. Furthermore, we acquired the immune therapy-related datasets, including the Alexandra cohort and GSE78220 from the previous study [24] and the GEO database (https://www.ncbi.nlm.nih.gov/gds) [25], respectively.

2.2. Differential expression genes (DEGs) screening

We first conducted the differential expression analysis in the KIRC dataset on the basis of the "limma" R package (version: 3.52.1). The Benjamini-Hochberg method was used to adjust the P-value. Then, we abstracted the log2(fold change) (also named logFC) and adjusted the p-value of RNA regulators from the results. We referred to the regulators with absolute logFC >0.5 and adjusted p-value <0.05 as differential expression RNA regulators in KIRC.

2.3. Identification of prognosis-related RNA regulators

We matched the mRNA expression of RNA regulators (PRR) and clincal survival outcomes based on their own unique patient ID. Then, the univariate Cox regression analysis was performed to determine the prognosis-related RNA regulators (PRR) based on the "coxph" R function from the "survival" R package. The univariate Cox regression model is a proportional hazards model, which assumes that each factor does not vary according to the change of time. Then, the function generates two important results, including

hazard ratio (HR) and p-value, which could used to determine whether a regulator is risky or protective. In general, the regulators with p-value <0.05 and hazard ratio (HR) > 1 were regarded as risky regulators, while those with p-value <0.05 and HR < 1 were regarded as protective regulators. Then, based on the ideal cut-off value determined by the "surv_cutpiont" function from the "survminer" package (version: 0.4.9) per gene, the data was separated into high and low-expression groups. The "surv_cutpoint" function could determine the optimal cutpoint for one or multiple continuous variables at once, using the maximally selected rank statistics from the 'maxstat' R package. This is an outcome-oriented methods providing a value of a cutpoint that correspond to the most significant relation with outcome. The Kaplain-Meier survival curve was further depicted, and the log-rank test was performed to estimate the significance between high and low-expression groups.

2.4. Cross-talk between RNA regulators

The prognosis-related RNA regulators (PRR) were submitted to the string websites **(https://string-db.org/) (Version: 12.0)**. STRING is a Core Data Resource as designated by Global Biodata Coalition and ELIXIR, which could be utilized to analyze the functional protein association networks. By selecting the "Multiple proteins" channel and "homo sapien" organism, the protein-protein interaction (PPI) of PRR could be analyzed and a network diagram could be depicted through the website. Then, the mRNA expression of PRR in TCGA KIRC tumor tissues was extracted to conduct the co-expression analysis based on the "rcorr" R function from the "Hmisc" R package. The co-expression analysis used the Pearson method, and Pearson correlation coefficients (PCC) were calculated to show the correlation between two RNA regulators. Absolute PCC >0.3 and P-value <0.05 were referred to as a mediate correlation between two variables, while absolute PCC >0.6 and P-value <0.05 were referred to as a strong correlation between two variables.

2.5. Construction of prognosis-related RNA regulators index (PRRI)

The KIRC dataset was split into a training cohort and a testing cohort based on the ratio of 7:3. Then, the lasso-cox regression analysis was performed to screen variables further and generate a regression coefficient per gene. The lasso regression is a compression estimation, which could refine the model by constructing a penalty function that compresses some coefficients and sets some coefficients of variables to zero. Based on the rationale, four regulators were further determined, while other regulators were expelled due to their coefficients being zero. Then, the prognosis-related RNA regulators index (PRRI) was established by calculating a sum of coefficient per gene multiply the expression of these genes. The function is as follows:

$$\mathrm{PRRI} = \mathrm{sum}(\mathrm{Coef_i}{*}\mathrm{Expression_i})$$

Among these, Coef represents the lasso-cox coefficient of the regulator, Expression represents the mRNA expression of the regulator, and i indicate each one of the determined regulators. We further used the PRRI to predict the overall survival of KIRC patients. We applied the Kaplian-Meier survival curve to show the difference between the high PRRI and low PRRI groups, the time-dependent ROC curve to estimate the predictive accuracy of PRRI on 3-/5-/7 prognosis, and heatmap to demonstrate the expression situation of four RNA regulators. All these analyses were conducted in KIRC training, KIRC testing, KIRP, and E-MTAB-1980 cohorts so that we could verify the practicality of PRRI.

2.6. Evaluation of PRRI

We further proceed to evaluate the PRRI by utilizing other clinical indexes, such as stage, grade, age, and gender. By observing the PRRI alteration among different clinical variables through a *t*-test, we could identify the correlation between PRRI and clinical variables. Furthermore, we separated the clinical data into different clinical subgroups. Then, the sample was split into high and low PRRI groups per subgroup; survival curves were depicted to show the prognostic differences. Finally, the PRRI and other clinical variables were merged to carry out multivariate Cox regression to determine the independent prognostic factors.

2.7. Nomogram model construction and evaluation

The prognosis-related variables (including PRRI, age, gender, histological grade, and pathological stage) were determined by univariate Cox regression analysis; these variables were submitted to multivariate Cox regression analysis based on the "survival" R package. Then, the model of multivariate Cox regression was submitted to the "step" R function to perform a stepwise regression analysis to screen variables deeply based on the minimum Akaike information criterion (AIC). Then, the variables selected by stepwise regression were used to erect the nomogram model. We applied the calibration to evaluate the accuracy of the nomogram model. The time-dependent ROC model was also performed to estimate the predictive efficacy of the nomogram model compared with other clinical variables in the 3-/5-/7-year prognosis of the patients based on the "survivalROC" R package (version: 1.0.3.1). Decision curve analysis was conducted, and the diagrams were depicted to show the net benefit of PRRI and other variables in predicting a 3-/5-/7-year prognosis. Finally, we constructed the risk score in the light of the nomogram and depicted a survival curve to show the prognostic difference between high and low-risk groups.

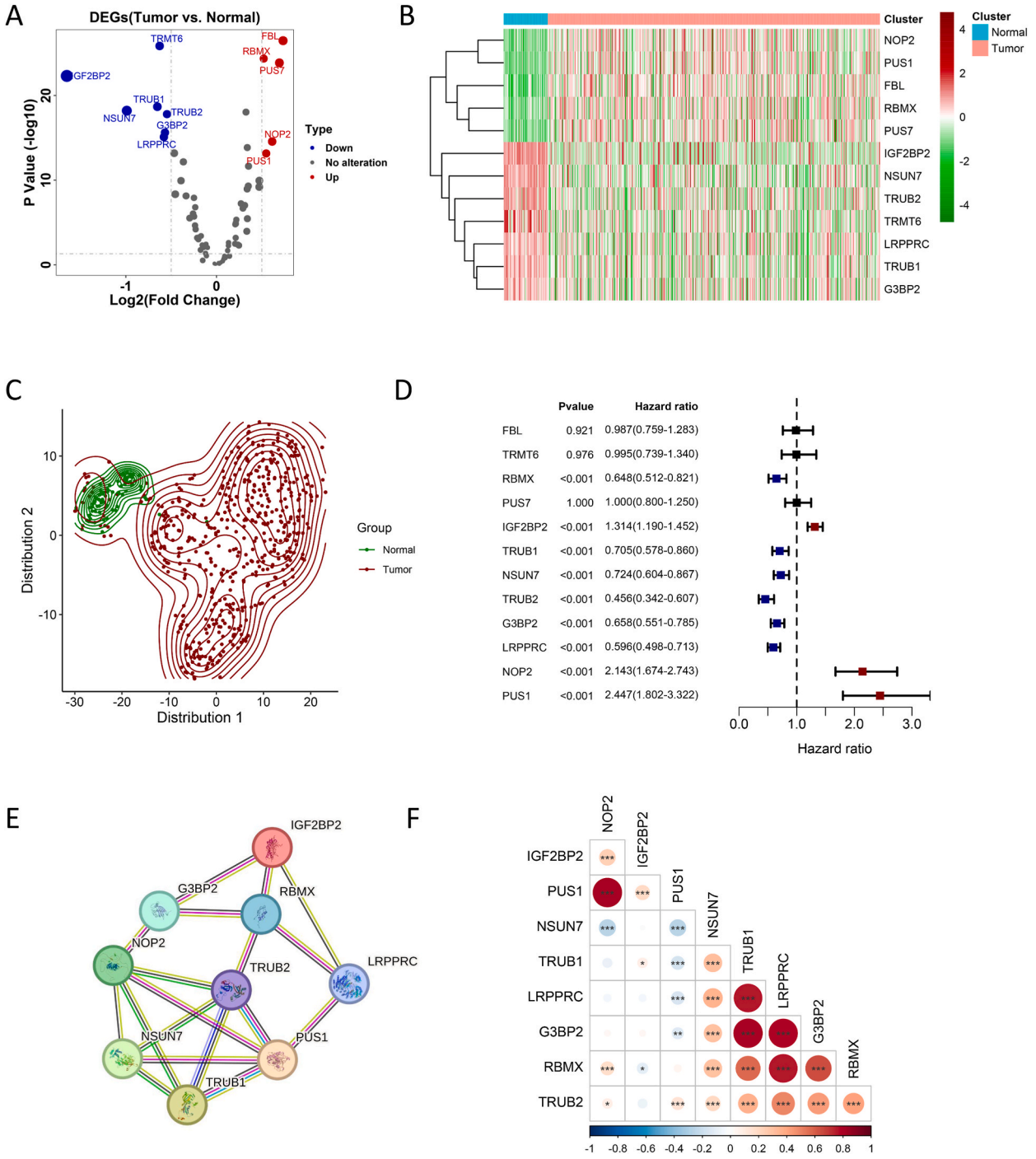

Fig. 1. The identification of prognosis-related RNA regulators (PRR). (A) The volcano plot shows the expression alteration of RNA regulators in KIRC; the red dot represents the up-regulated genes, and the blue dot represents the down-regulated genes. **(B)** The heat map shows the mRNA expression situation of regulators in tumor and normal tissues; the red represents high expression, and the blue represents low expression. **(C)** The two-dimensional density map depicted based on the T-SNE methods shows the distribution of tumor and normal samples in the light of the expression of regulators. **(D)** The forest plot shows the prognosis-related RNA regulators (PRR) of KIRC; the red shows the risky regulators, while the blue shows the protective regulators. **(E)** The network diagram shows the protein-protein interaction of PRR. **(F)** The heat map shows the co-expression relationship among the PRR. The asterisk represents a significant relation between the two PRRs.

2.8. Mechanism exploration

The co-expression genes of RNA regulators were submitted to The Database for Annotation, Visualization and Integrated Discovery (DAVID) website (**https://david.ncifcrf.gov/**) so that function enrichment could be analyzed. By uploading the gene list, including co-expression genes, and selecting the official gene symbol identifier and homo sapien species, multiple functional enrichment results would bring out on the website. The interesting items (such as GO and KEGG pathways) could be downloaded to depict diagrams to show the enrichment situations. Then, we downloaded the gene sets including 50 hallmark pathways, from the MsigDB database (https://www.gsea-msigdb.org/gsea/msigdb). Then, the 50 hallmark pathway activity score per sample could be calculated by gene set variation analysis (GSVA) by sending in gene sets and mRNA expression profile of the KIRC dataset to the "GSVA" R package (version: 1.44.5). The correlation between PRRI and pathway activity was computed, and the bubble plot was portrayed to show the correlation. While exploring the mechanisms of the high PRRI and low PRRI groups, we first analyzed the differential expression genes (DEGs) between these two groups, and then the DEGs ranked by logFC were submitted to the "clusterProfiler" R package (version: 4.4.4) so that molecular function and biological progression could be analyzed. In addition, the samples of KIRC mRNA expression data were ranked through PRRI; the samples with high PRRI were put before the samples with low PRRI. Then, the ranked mRNA expression data was submitted to Gene Set Enrichment Analysis (GSEA) software (Version: GSEA-4.0.3) to analyze differentially enriched pathways; the parameter - 1000 permutation, no collapse, and phenotype were selected during this performance.

2.9. Evaluation of tumor immune infiltration and immune therapy

For the calculation of tumor immune infiltration levels, we used two methods - the "xCell" R package (version: 1.1.0) and the single-sample gene set enrichment (ssGSEA) method based on the "GSVA" R package. We submitted the mRNA expression profile of KIRC to the function "xCellAnalysis" R function from the "xCell" R package, and then the immune cell infiltration level per sample will be computed. Then, we obtained the gene sets representing twenty-four types of immune cells from the published research [26]. The gene sets and expression profiles were submitted to the "GSVA" R package to count the infiltration levels of immune cells based on the ssGSEA method. Then, the immune infiltration levels were normalized by function as follows:

$$\text{Immune infiltration level} = \frac{x - \min(x)}{\max(x) - \min(x)}$$

Among these, x indicates the mRNA expression profile of TCGA KIRC. Furthermore, we used the "CIBERSORT" to evaluate the fraction of 22 types of immune cells. For immune therapy prediction, we used a public website - Tumor Immune Dysfunction and Exclusion (TIDE), to predict the potential relation between PRRI and immune therapy response [27]. Then, we used the immune therapy datasets for further validation.

2.10. Statistic analysis

All analysis are carried out with R software (version: 4.2.2). The Kaplain-Meier curve was portrayed to show the survival probability of two groups; the statistical significance was estimated by the log-rank test. The Pearson correlation coefficient (PCC) based on the Pearson method was used to estimate the correlation between the two variables. The T-test was utilized to analyze the difference between two continuous variables, and the chi-square test was used to assess the distribution distinction of contingency table data.

3. Results

3.1. Identification of prognosis-related RNA regulators (PRRs)

The specific workflow of this study is shown in Flow chart. We first performed differential expression analysis to screen the differential expression RNA regulators by comparing the whole genome expression of 535 tumors and 72 normal samples in the TCGA KIRC dataset. Twelve differential expression genes (DEGs) were finally determined (Fig. 1A). *NOP2*, *PUS1*, *FBL*, *RBMX*, and *PUS7* show upregulation in tumor tissues. *IGF2BP2*, *NSUN7*, *TRUB2*, *TRMT6*, *LRPPRC*, *TRUB1*, and *G3BP2* down-regulate in tumor tissues (Fig. 1B). T-SNE analysis reveals that the expression characteristics of these RNA regulators are different in normal and tumor tissues (Fig. 1C). To screen the prognosis-related RNA regulators (PRRs), we conducted the univariate Cox regression analysis. The results reveal that *RBMX*, *IGF2BP2*, *TRUB1*, *NSUN7*, *TRUB2*, *G3BP2*, *LRPPRC*, *NOP2*, and *PUS1* are correlated with prognosis of KIRC patients (Fig. 1D). Among these, *IGF2BP2*, *NOP2*, and *PUS1* show a risky factor (HR $>$ 1 & P-value $<$0.05), and the patients with high expression of these genes show a worse outcome (Figure S1). While others prove to be protective factors (HR $<$ 1 & P-value $<$0.05), the patients with high expression of these genes show better clinical outcomes. By analyzing the protein-protein interaction between these nine PRRs, we found that they possess a complex relationship (Fig. 1E). In addition, *TRUB1*, *LRPPRC*, *G3BP2*, *RBMX*, and *NSUN7* show a positive correlation with each other. PUS1 shows a negative correlation with *NSUN7*, *TRUB1*, *LRPPRC*, *G3BP2*. *NOP2* is positively related to *IGF2BP2*, *RBMX*, and *PUS1* but negatively related to *NSUN7* (Fig. 1F).

3.2. Potential function and mechanisms of PRRs

To explore the function of PRRs, we performed the Pearson correlation analysis. The concrete progression is shown in Fig. 2A. Specifically speaking, we first analyzed the correlation between the mRNA expression of PRRs and the whole genome using the Pearson method. The p-value was adjusted by false discovery rate (FDR). The absolute Pearson correlation coefficient >0.6 and adjusted p-value <0.05 are utilized as a threshold to identify the genes that are highly co-expressed with PRRs. Finally, the identified genes were submitted to the functional enrichment website - DAVID. The results revealed that this gene might be associated with some biological functions, such as regulation of transcription DNA-templated; ubiquitin-dependent protein catabolic process; regulation of transcription from RNA polymerase II promoter; protein transport; protein ubiquitination, etc.; molecular functions, such as protein binding, RNA binding, metal binding, ubiquitin-protein transferase activity, ATP binding, etc.; cell components, such as nucleoplasm, nucleus, cytosol, cytoplasm, mitochondrion, etc.; KEGG pathways, nucleocytoplasmic transport, ubiquitin-mediated proteolysis, autophagy animal, mRNA surveillance pathway, etc (Fig. 2B–E). We further calculated the correlation of these PRRs and the activity of cancer-related pathways and found that these PRRs play different functions in KIRC. For instance, *NOP2* positively correlates with G2M checkpoint, E2F targets, and MYC target V1/V2, indicating that *NOP2* might function in tumors by regulating these cell cycle-related pathways (Fig. 2F).

3.3. PRRs risk model construction

We then matched the RNA regulators' expression profile and clinical data, and then the samples were separated into the training cohort and testing cohort. Based on the lasso-cox regression analysis, the RNA regulators index model was further established in the training cohort (Fig. 3A). The results revealed that when the number of PRRs was four, the partial likelihood of deviance was minimal (Fig. 3B). Based on the lasso coefficients of these four genes, the risk model was finally constructed according to the equation as follows:

$$\text{PRRI (PRRs index)} = 0.2202288*\textit{IFG2BP2} - 0.4756218*\textit{TRUB2} - 0.2745814*\textit{LRPPRC} + 0.5061372*\textit{NOP2}$$

In the training cohort, the patients were separated into high-PRRI and low-PRRI groups based on the optimal cut-off value. The Kaplain-Meier survival curve reveals that high PRRI patients show a lower survival probability than low PRRI patients (Fig. 3C). The predicted accuracy of PRRI on KIRC prognosis is over 70 % in 3-/5-/7-year survival (AUC at 3 years = 0.7132, AUC at 5 years = 0.7220, AUC at 7 years = 0.7283). Among these, *TRUB2* and *LRPPRC* are highly expressed in the high PRRI patients, while *IGF2BP2* and *NOP2* are highly expressed in the low PRRI patients. We then conducted the same analysis in the KIRC testing cohort, E-MTAB-1980, and KIRP cohort. The results are consistent with the findings analyzed by the KIRC training cohort. The predicted accuracy is relatively high in these three cohorts (For testing cohort: AUC at 3 years = 0.7141, AUC at 5 years = 0.7403, AUC at 7 years = 0.7305; For E-MTAB-1980 cohort: AUC at 3 years = 0.7038, AUC at 5 years = 0.7385, AUC at 7 years = 0.7143; For KIRP cohort: AUC at 3 years = 0.6203, AUC at 5 years = 0.6365, AUC at 7 years = 0.6941) (Fig. 3D–F).

3.4. Association of PRRI and clinic

We further analyzed the relationship between PRRI and clinic in the KIRC dataset, and we found the advanced pathological stage and histological grade mainly harboured in high PRRI groups, while the age and gender show no significant differences between high and low PRRI groups (Fig. 4A and B). In E-MTAB-1980 datasets, male patients, higher grade and stage harbored in high PRRI groups, while age still shows no correlation with PRRI (Figs. S2A–B). By dividing the clinical samples into high and low PRRI groups based on the ideal cut-off value in different clinical sub-groups (i.e., age was separated into two sub-groups: age >60 and age ≤60, and then, the different clinical sub-groups were separated into high and low PRRI groups). We found that no matter what the sub-groups were, patients with high PRRI invariably showed a lower survival probability than patients with low PRRI (Fig. 4C, Figure S2 C). These results revealed that PRRI might be practical for predicting the prognosis of patients who are harbored in different clinical subgroups.

3.5. Establishment of nomogram model

We then utilized the PRRI as well as other clinical variables, including pathologic stage, grade, gender, and age, to conduct a multivariate Cox regression analysis. We found that PRRI, pathologic stage, grade, and age are independent prognostic factors for KIRC patients (Fig. 5A). Based on the multivariate Cox regression model, a nomogram was established by applying histological grade, pathologic stage, age, and PRRI (Fig. 5B). Based on the patient's characteristics, total points could be calculated by integrating each point per variable; different total points represent different 3-/5-/7-year survival probabilities for the patient. The calibration curve reveals that the nomogram model could predict the prognosis of the patients well (Fig. 5C). In addition, nomogram model shows a highest predictive accuracy (i.e., For 3 years, AUC of nomogram = 0.8146, AUC of age = 0.5704, AUC of gender = 0.4828, AUC of grade = 0.7033, and AUC of stage = 0.7808; For 5 years, AUC of nomogram = 0.7736, AUC of age = 0.5834, AUC of gender = 0.4806, AUC of grade = 0.6713, and AUC of stage = 0.7089; For 7 years, AUC of nomogram = 0.7522, AUC of age = 0.6064, AUC of gender = 0.4952, AUC of grade = 0.6592, and AUC of stage = 0.6756) (Fig. 5D). Decision curve analysis (DCA) analysis reveals that the nomogram model could reach the highest clinical benefit compared with other clinical variables (Fig. 5E). In terms of nomogram, a risk score was constructed, and the patients were separated into high and low-risk groups according to the cut-off value. The Kaplain-Meier

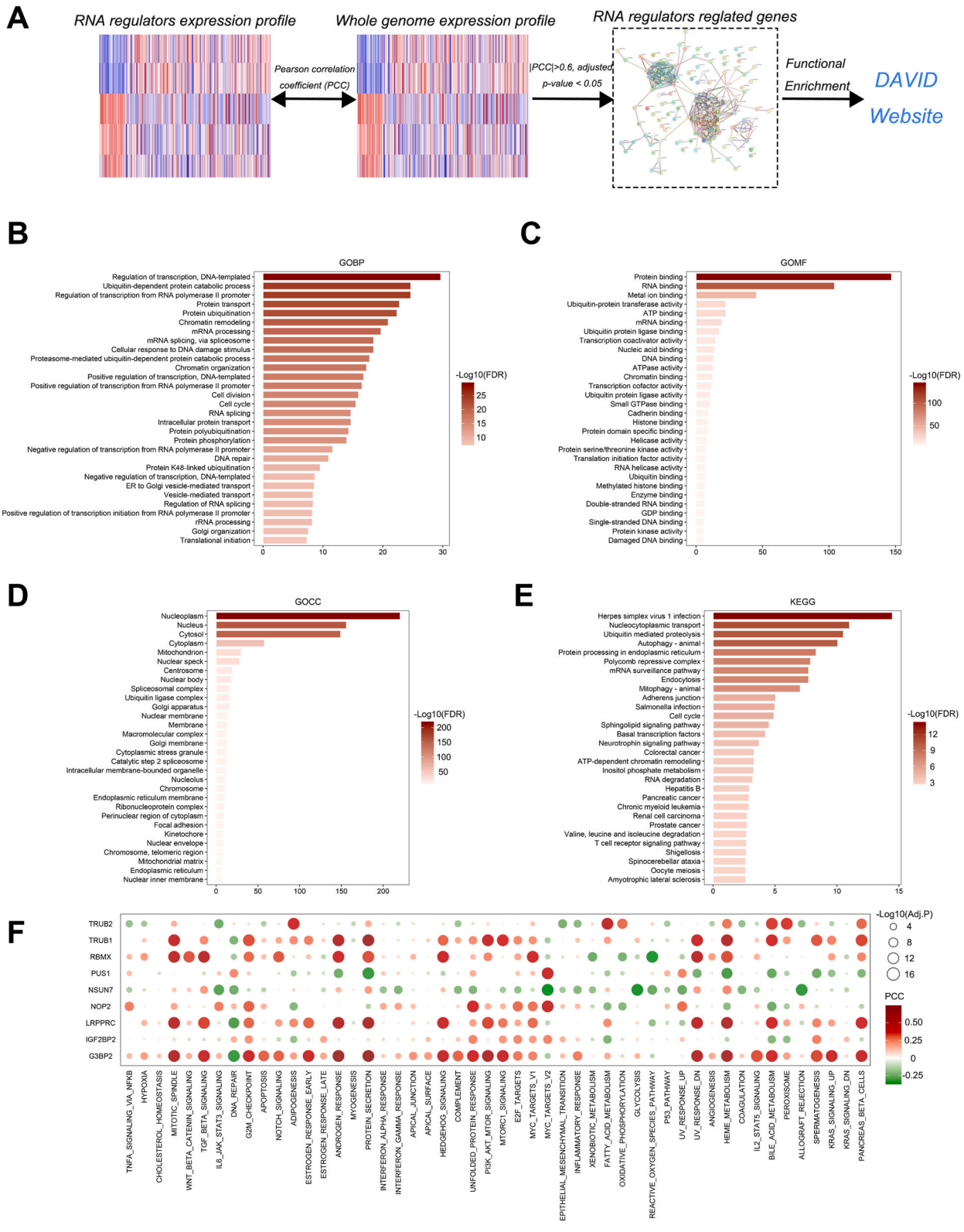

(caption on next page)

Fig. 2. Function enrichment and mechanism exploration. (A) The schematic diagram shows the progression of function enrichment analysis. **(B–E)** Barplots show the biological progression, molecular function, cell component, and KEGG pathways of co-expression genes of PRR. **(F)** The heat map shows the correlation between PRR and activity score of 50 cancer-related hallmark pathways in the KIRC dataset. The red represents a positive correlation, while the blue represents a negative correlation. The size of the dot represents the significance.

survival curve shows a dramatically significant survival difference between the high and low-risk groups, revealing that the nomogram could discriminate the patients with different clinical outcomes (Fig. 5F).

3.6. The function enrichment analyses between high PRRI and low PRRI

To understand the potential mechanisms between high PRRI and low PRRI, we conducted the differential expression analysis between high and low PRRI groups. The differential different genes were subjected to biological progression (BP) and molecular function (MF) analysis based on the "clusterprofiler" R package. For BP, regulation of systemic arterial blood pressure by renin-angiotensin, acyl-CoA metabolic process, thioester metabolic process, and regulation of systemic arterial blood pressure shows a low enrichment in high PRRI group, while regulation of T cell migration, regulation of lymphocyte migration, antibacterial humoral response, negative regulation of leukocyte apoptotic process, antimicrobial humoral response highly enriched in high PRRI group (Fig. S3A). For MF, solute: sodium symporter activity, phosphoric diester hydrolase activity, monocarboxylic acid transmembrane transporter activity, sodium ion transmembrane transporter activity, organic hydroxy compound transmembrane transporter activity show a low enrichment in the high PRRI group, while immunoglobulin receptor binding, antigen binding, chemokine activity, chemokine receptor binding, serine-type endopeptidase inhibitor activity highly enriched in high PRRI group (Fig. S3B). We further submitted the mRNA expression profile of KIRC and cancer hallmark pathway gene sets in gene set enrichment analysis (GSEA) software (Version: GSEA-4.0.3) and found several hallmark pathways, such as xenobiotic metabolism, androgen response, peroxisome, fatty acid metabolism, P13K_AKT_MTOR signaling, adipogenesis, protein secretion, bile acid metabolism, oxidative phosphorylation, and heme metabolism show a low enrichment in high PRRI group (Fig. S4).

3.7. Immune therapeutic prediction of PRRI

We further analyzed the mutation characteristics of high PRRI and low PRRI groups. The results show that missense mutation and SNP are the most prevalent variation types (Fig. S5A). However, the mutation burden between high and low PRRI groups shows no significant difference, with 85.23 % alteration in the low-risk group and 85.71 % alteration in the high-risk group (Fig. 6A and Fig. S5A). Intriguingly, when we analyzed the alteration of clinically actionable genes in the high and low PRRI groups, we found more mutations of clinically actionable genes (84.76 %) in the high PRRI group than in the low PRRI group (Fig. S5B). For example, we observed that *BAP1* and *MTOR* show a higher mutation rate in the high PRRI group than in the low PRRI group. From the results of the mechanism enrichment analysis above, we found several immune-related pathways highly enriched in the high PRRI group, such as regulation of T cell migration. We reflected that the immune system might play an important part in causing the prognostic difference between the high PRRI and the low PRRI group, so we further observed the correlation between the immune system and PRRI. We first observed the mRNA expression of several immune-related genes in high and low PRRI groups (Fig. 6B). Apart from *CD274*, we found that *PDCD1*, *CTLA4*, *CD27*, *TIGIT*, and *LAG3* showed a higher expression in the high PRRI group than in the low PRRI group. The high PRRI group showed a higher immune score and microenvironment score and a lower stroma score (Fig. 6C). In addition, pro-tumor immune cell - fibroblasts and anti-tumor immune cells $CD8^+$ T-cells and NKT cells show significant activation in the high PRRI group. We further observed the activity score of 24 immune cells and a fraction of 22 immune cells in high and low PRRI groups (Fig. 6D and E). The results show that lots of immune cells are differentially altered in these two groups. Interestingly, Tregs activity and fraction are higher in the high PRRI group than in the low PRRI group, which is consistent with the results of function mechanism analyses. We further analyzed the correlation between PRRI and immune cell activity/fraction and found that PRRI highly correlated with Tregs' activity and fraction compared to anything else (For Tregs' activity, PCC = 0.3931, P-value < 2e-16; for Tregs' fraction, PCC = 0.4056, P-value < 2e-16) (Figs. S6A–D). These results indicate that high PRRI might promote Tregs' enrichment and infiltration. Considering that Tregs could inhibit immune response so that an immune therapeutic resistance could be caused, we presumed that the patients in the high PRRI group might not be sensitive to immune therapy. This was indeed the case; through the TIDE analysis, we found that most of the non-responders harbored in the high PRRI group, while most of the responders harbored in the low PRRI group (Fig. 6F). What is more, the patients who turned out to be the no responders showed a higher PRRI than the responders (Fig. 6G). In two anti-PD1 datasets, we also observed that the patients in the high PRRI group showed worse clinical outcomes. However, due to the small number of samples of these two datasets, the difference between high and low PRRI groups does not show statistical significance (Figs. S7A and B). Nevertheless, we observed that most of the patients in the high PRRI group harbored in the SD/PD (SD, stable disease; PD, progression disease) group, while most of the patients in the low PRRI group located in CR/PR (CR, compete for response; PR, partial response) group (Figs. S7C and D), indicating that patients with high PRRI might predict resistance of immune therapy to some degree.

4. Discussion

Renal cell carcinoma (RCC) is one of the most routinely diagnosed urological cancers, which causes large sums of patients to come

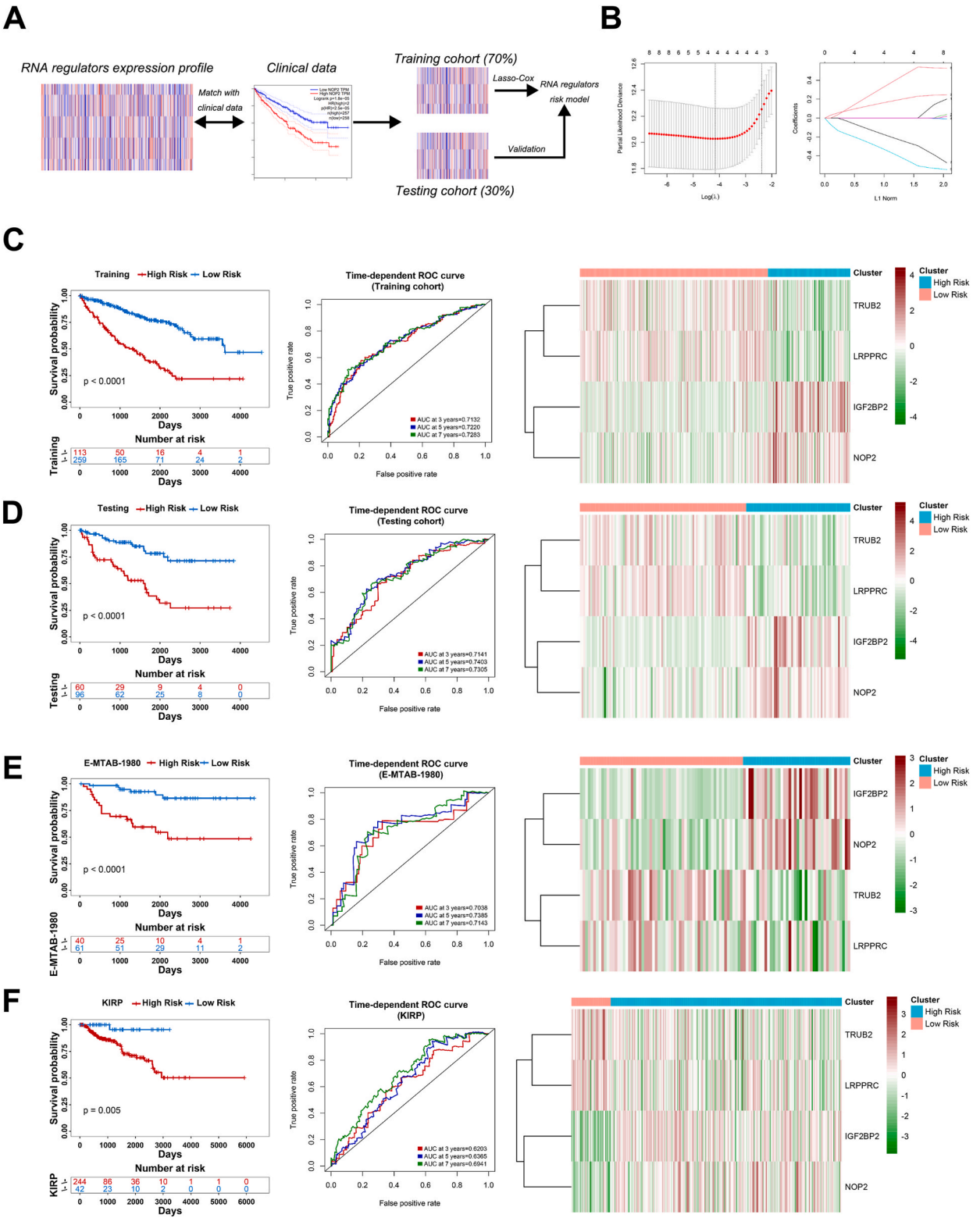

(caption on next page)

Fig. 3. PRR index (PRRI) construction and risk model evaluation. (A) The schematic diagram shows the progression of the construction of PRRI. **(B)** These two diagrams show the progression of lasso-cox regression. **(C–F)** The Kaplain-Meier survival curves show the survival probability of high and low PRRI groups in the training cohort, testing cohort, E-MTAB-1980 cohort, and KIRP cohort. The time-dependent ROC curves show the predictive accuracy of PRRI on 3, 5, and 7 years of overall survival. The heatmaps show the expression differences of PRR that were used to construct the PRRI in high and low PRRI groups; the red represents high expression, and the green represents the low expression.

to death per year [28,29]. Though there are various therapeutic methods, such as surgery, chemotherapy, radiotherapy, and immunotherapy, kidney cancer is still faced with many challenges [30]. Approximately 40 % of patients with advanced cancer ultimately develop metastasis and cause poor clinical outcomes [31]. So, it is essential to determine the biomarkers that are suitable to predict the prognosis of patients and develop new clinical potential targets. Recent research has shed attractive light on RNA modification, which might play an essential role in cancer and could be referred to as potential drug targets [12]. Several RNA-modifying proteins are misregulated in human cancer and are implicated in the responses of tumor cells to oxidative stress, DNA damage and drug exposure occurring (such as chemotherapy and radiotherapy) [32]. RNA modification mainly depends on specific RNA enzymes, also known as regulators. Unlike other cancer drivers, these regulators are not commonly altered in cancer, but cancer cells often use these enzymes to maintain the growth and development of tumors. Therefore, they are considered potential targets, which is a reasonable strategy against cancers. Though research revealed that some RNA regulators could affect biological behavior and function, for example, the expression of the m6A-dependent gene (*METTL3/METTL14*) is controlled by Von Hippel Lindau (*VHL*) tumor suppressor in renal tumorigenesis [33], the concrete role of other RNA modifications that had once been identified to be associated with tumors had not found its way into this type of tumour. Therefore, exploring the alteration and function of multiple types of RNA regulators in kidney cancer could provide a theoretical foundation for tumor target therapy based on RNA regulators. What is more, though many gene models are constructed to predict outcomes of kidney cancer patients [21,34,35], the model based on RNA modification regulators has not been determined for prognosis and therapy prediction.

To screen potentially important RNA regulators, we first conducted differential expression and uni-variate Cox regression analysis based on 82 identified RNA regulators in the TCGA KIRC dataset. We identified 9 RNA modification regulators, which are not only differentially expressed in KIRC but also turn out to be correlated with the prognosis of the patients. Several genes have been found to play an essential role in kidney cancer. For example, Circ-TNPO3 could bind to IGF2BP2 protein to inhibit the progression of clear cell renal cell carcinoma (ccRCC) [36]. *ZNF677* acts as a tumor suppressor and is frequently silenced by m6A modification in RCC; the m6A-modified coding sequence (CDS) of *ZNF677* could influence its stability by combining with *IGF2BP2* [37]. The upregulation of *PUS1* also causes increasing migration and invasion of RCC cells, while its downregulation can result in the opposite effects [38]. These results suggest that our screened progression is reasonable, even though other genes have not found their concrete functions and effects in kidney cancer. We further conducted the function enrichment analysis. After submitting the co-expressed genes of these 9 regulators to a public website, we found that these genes mainly enriched in multiple RNA regulation-related pathways, which is consistent with the feature of RNA regulators [12]. Intriguingly, we found that these nine RNA regulators appear to have a positive or negative correlation with different cancer-related hallmark pathways, which provide a foundation and potential routine for exploring concrete mechanisms of these regulators for future researchers. Through the machine learning algorithm - lasso-cox regression, we further determined 4 core regulators, including *TRUB2*, *LRPPRC*, *IGF2BP2*, and *NOP2*, and constructed the risk model called PRRI to predict the clinical outcome of RCC patients. We found that high PRRI patients show poorer outcomes than low PRRI patients in three datasets and different clinical subgroups, indicating that PRRI is practical for patients with RCC. When a patient was determined to have RCC, we could inspect the expression of these genes and calculate his PRRI; then, we could deduce his potential prognosis. Notably, *IGF2BP2* and *NOP2*, which have been proven to regulate m6A and m5C modification, respectively, show high expression in high PRRI groups. Apart from kidney cancer, *IGF2BP2* has been proven to act as a pro-tumor factor in many types of cancer, for it not only could stabilize other genes to promote cancer metastasis but also can degrade RNA transcript of the gene to promote cancer progression [39–41]. *NOP2/NSUN1* is overexpressed in a wide variety of cancers, and its expression is closely related to progression, poor prognosis, and therapy resistance, revealing that it might be a promising tumor therapeutic target [42–46]. It seems that targeting these two regulators for patients who have been determined in high PRRI groups might be a selective therapeutic strategy against kidney cancer. However, such speculation still needs to be validated in future pre-clinical research. Previous research used multivariate Cox regression analysis to determine potential independent prognostic factors [47–49]. In our analysis, we used the clinical variables as covariates to explore the importance of PRRI; the results reveal that PRRI is still a significant prognostic factor and is not affected by other clinical variables, verifying its independence.

Considering that the immune-related pathways are differentially enriched in high and low PRRI patients, we further explore the relationship between PRRI and immune systems in kidney cancer. Intriguingly, we found that most immune-related genes are highly expressed in the high PRRI group, indicating that patients with high PRRI are liable to undergo immune escape. Furthermore, we found Tregs highly enriched in the high PRRI group, and PRRI shows a highly positive correlation with the activity score of Tregs. In multiple types of cancer, increased numbers of Tregs are correlated with worse prognosis [50–53]. In addition, Tregs have been proven to be a pro-tumor immune cell. For they could not only inhibit the activity of the anti-tumor cell but also promote immune escape [54–56]. Tregs' deletion could promote available anti-tumor immunity, especially if Treg cells are depleted systemically [57,58]. The PRRI is positively correlated with Tregs' activity, indicating indirectly that high PRRI patients might suffer from the activation of high Tregs' infringement and cause poor prognosis and therapy effects. In other immune therapeutic datasets, most of the patients in the high PRRI group turned out to be non-responders. So, based on these results, we speculate that patients with high PRRI might not benefit from immune therapy. For these patients, precaution is necessary. During their immune therapy, another therapeutic strategy should be

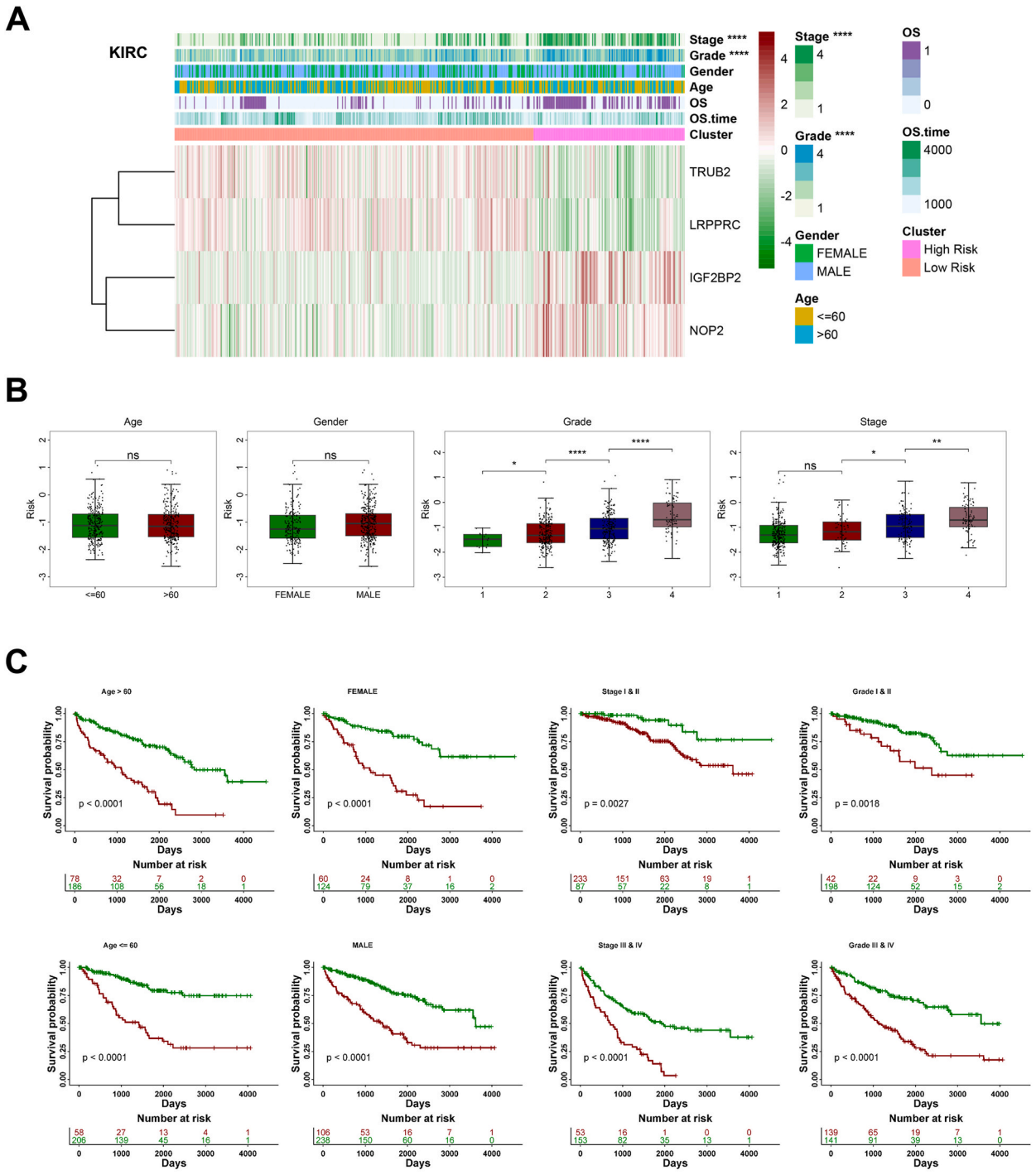

Fig. 4. The relationship between PRRI and clinic in the KIRC dataset. (A) The heatmap shows the expression comparison of PRR, which was used to construct the PRRI in high PRRI and low PRRI groups, and the distribution of other clinical variables (such as stage, grade, gender, and age) in high and low PRRI groups. The asterisk shows the statistical significance analyzed by the chi-square test. **(B)** Boxplots show the value of PRRI in different groups of age, gender, grade, and stage. **(C)** In different clinical subgroups, age >60 and age ≤60, stage I/II and stage III/IV, male/female, grade I/II and grade III/IV, the samples were separated into high and low PRRI groups, then the survival curves show the survival rate between the two groups. *, $P < 0.05$; **, $P < 0.01$; ****, $P < 0.0001$; ns, no significance.

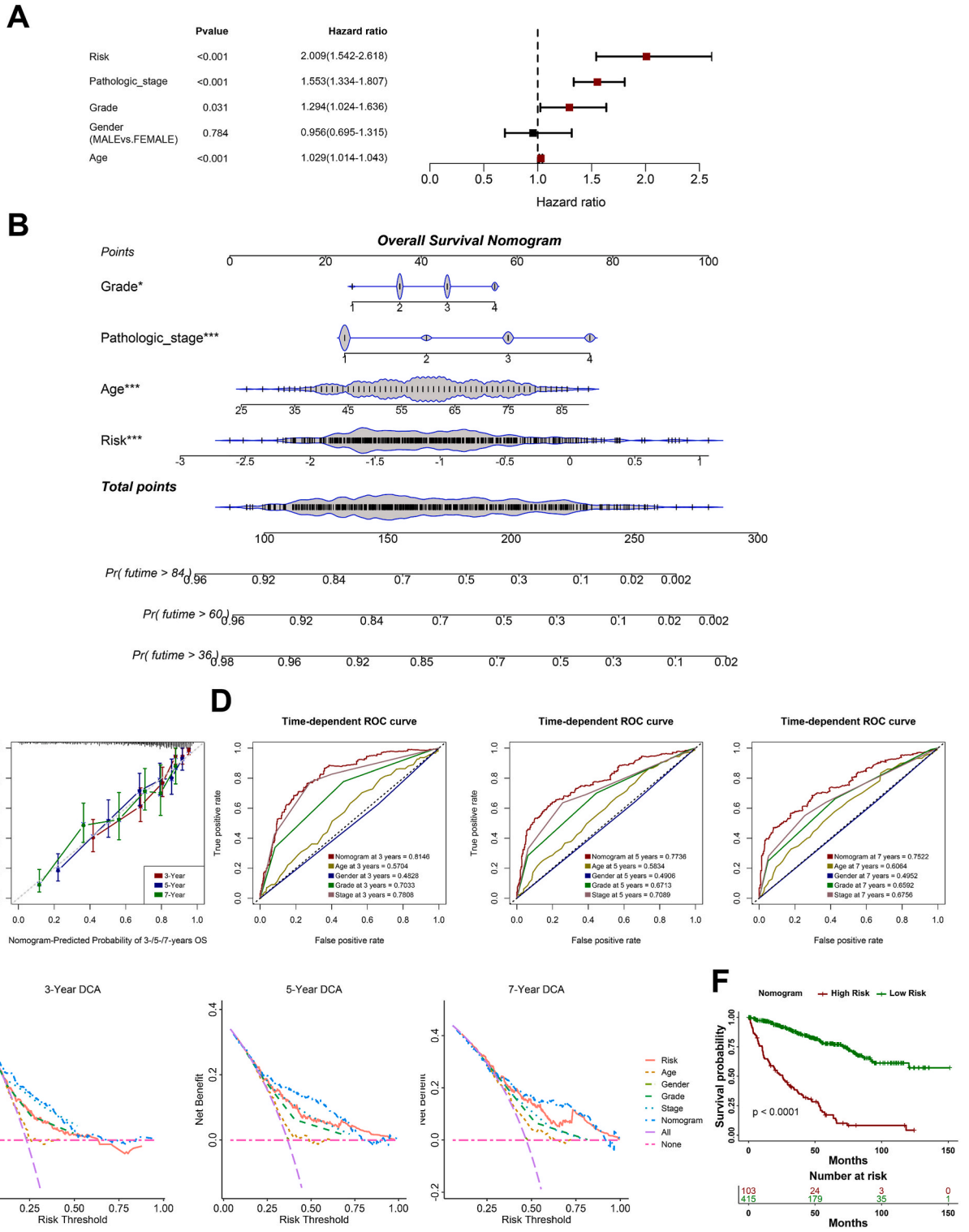

Fig. 5. Nomogram construction and model evaluation. (A) The forest plot shows the consequence of multivariate Cox regression analysis. **(B)** The nomogram plot shows the points per variable, and the total points correspond to survival rates of 3, 5, and 7 years. **(C)** The calibration curve shows the accuracy of the nomogram model. **(D)** The time-dependent ROC curve was depicted to compare the predictive efficacy of the nomogram model as well as other clinical variables at 3, 5, and 7-year survival. **(E)** The decision curve was depicted to analyze the net benefit of the nomogram model as well as other clinical variables. **(F)** The Kaplain-Meier survival curve was depicted to show the survival difference between high and low-risk groups that had been constructed and determined by the nomogram model.

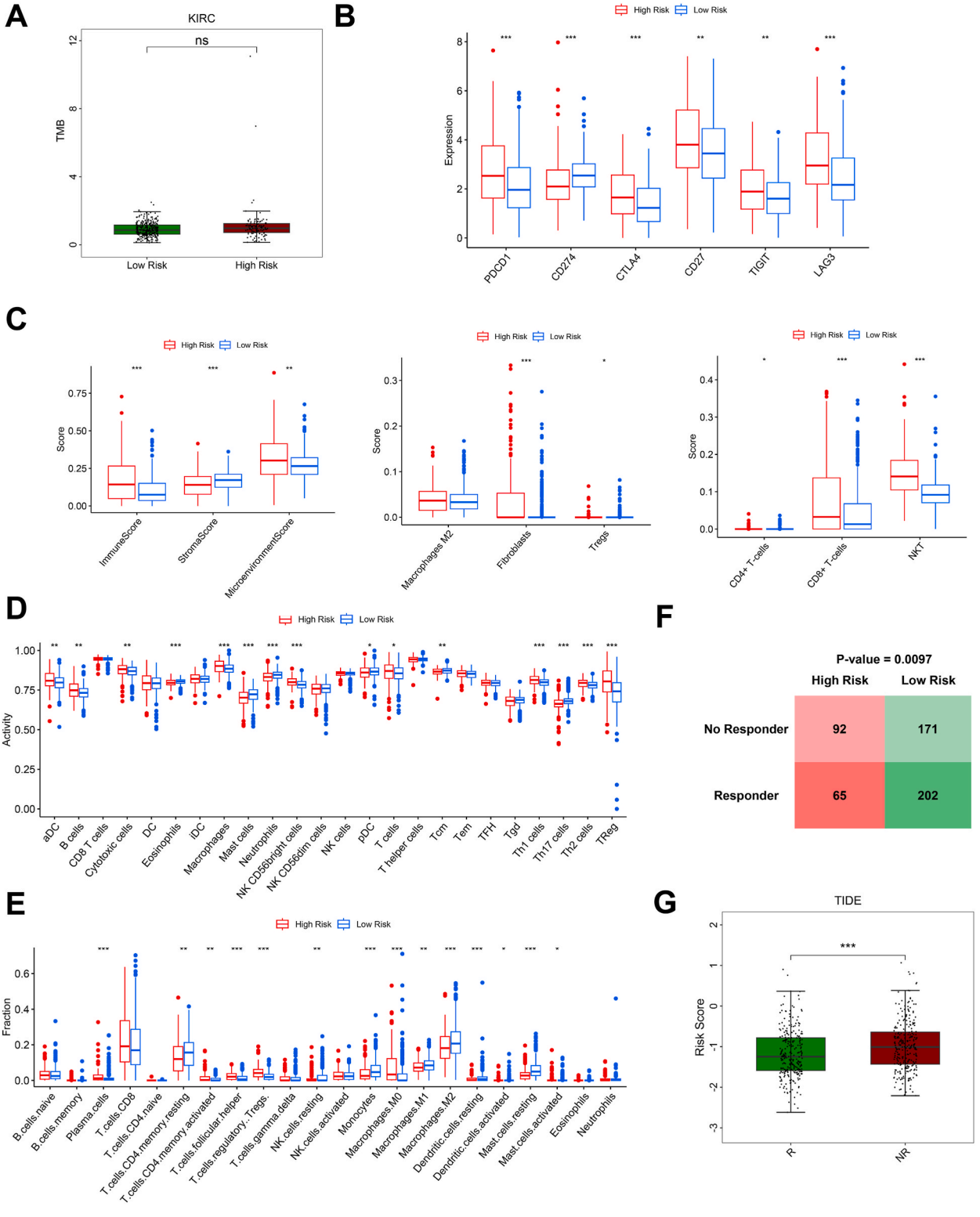

(caption on next page)

Fig. 6. Relationship between PRRI and tumor immune. **(A)** Tumor mutation burden in high and low PRRI groups. **(B)** Immune-relate gene expression in high and low PRRI groups. **(C)** Immune score, stroma score, microenvironment score, and activity of tumor microenvironment cells (including Macrophage M2, fibroblasts, Tregs, CD4+T cells, CD8+T cells, NKT cells) in high and low PRRI groups. **(D)** Activity differences of 24 immune cells in high and low PRRI groups. **(E)** Fraction of 22 immune cells in high and low PRRI groups. **(F)** The distribution of responder and no responder in high and low PRRI groups. **(G)** Boxplot shows the difference between PRRI in responders and non-responders. *, $P < 0.05$; **, $P < 0.01$; ***, $P < 0.001$; ****, $P < 0.0001$; ns, no significance.

allowed.

Several limitation should be mentioned in this study, even though our PRRI could predict prognosis and immune therapeutic response to some extent. This is retrospective studies and PRRI was constructed based on existing datasets, which lack of support of prospective data. Furthermore, though we systematically excavated the function and mechanisms of RNA regulators, which still lack of experiment validation to clarify these predictions.

In summary, we analyzed the expression and function of RNA modification regulators identified in kidney cancer and finally determined some essential genes used to construct the risk model to predict prognosis and immune response. More and more researchers have commenced studying the role of RNA modification, and we hope our predicted data might supply some information and foundations for further pre-clinical and clinical research.

Ethics approval and consent to participate

Not applicable.

Consent for publication

Not applicable.

Funding

Funding information is not available.

Availability of data and materials

The data and materials of this study can be found on public websites, including UCSC Xena (https://xena.ucsc.edu/), Arrayexpress (https://www.ebi.ac.uk/arrayexpress), GEO (https://www.ncbi.nlm.nih.gov/gds), string website (https://string-db.org/).

Clinical trial number

Not application, this research is based on public datasets, and there is no new data emerged.

CRediT authorship contribution statement

Gang Li: Writing – review & editing, Writing – original draft, Software, Methodology, Funding acquisition, Conceptualization. **Jingmin Cui:** Writing – review & editing, Writing – original draft, Resources, Formal analysis, Data curation, Conceptualization. **Shuang He:** Methodology, Investigation, Funding acquisition, Formal analysis. **Xiufang Feng:** Software, Resources. **Wenhan Li:** Visualization, Validation. **Tao Li:** Software, Resources. **Peilin Chen:** Writing – review & editing, Supervision, Methodology, Investigation, Funding acquisition, Conceptualization.

Declaration of competing interest

The authors declare that they have no known competing financial interests or personal relationships that could have appeared to influence the work reported in this paper.

Acknowledgments

Not applicable.

Appendix A. Supplementary data

Supplementary data to this article can be found online at https://doi.org/10.1016/j.heliyon.2024.e39021.

References

[1] Y. Mei, M. Yongzhen, R. Daixi, L. Shun, Z. Zhaoyang, X. Wei, Transfer RNA-derived small RNAs in tumor microenvironment, Mol. Cancer 22 (1) (2023) 32.
[2] W. Jie, G. Junshang, W. Yian, X. Fang, G. Jiayue, J. Xianjie, et al., EBV miRNAs BART11 and BART17-3p promote immune escape through the enhancer-mediated transcription of PD-L1, Nat. Commun. 13 (1) (2022) 866.
[3] X. Fang, Z. Kunjie, D. Su, H. Hongbin, Y. Liting, G. Zhaojian, et al., AFAP1-AS1: a rising star among oncogenic long non-coding RNAs, Sci. China Life Sci. 64 (10) (2021) 1602–1611.
[4] B. Pietro, S. Filip, R. Angana, C. Andrea, M. Sunandan, P. Elżbieta, et al., MODOMICS: a database of RNA modification pathways. 2021 update, Nucleic Acids Res. 50 (D1) (2021) D231–D235.
[5] A.R. Ian, E.E. Molly, P. Tao, H. Chuan, Dynamic RNA modifications in gene expression regulation, Cell 169 (7) (2017) 1187–1200.
[6] C. Kunqi, S. Bowen, T. Yujiao, W. Zhen, X. Qingru, S. Jionglong, et al., RMDisease: a database of genetic variants that affect RNA modifications, with implications for epitranscriptome pathogenesis, Nucleic Acids Res. 49 (D1) (2020) D1396–D1404.
[7] H. Jie, W. Jing-Zi, Y. Xiao, Y. Hao, Z. Rui, L. Hong-Cheng, et al., METTL3 promote tumor proliferation of bladder cancer by accelerating pri-miR221/222 maturation in m6A-dependent manner, Mol. Cancer 18 (1) (2019) 110.
[8] B. Konstantinos, Lieberman G. Eric, Biological roles of adenine methylation in RNA, Nat. Rev. Genet. 24 (3) (2022) 143–160.
[9] H. Liuer, L. Huiyu, W. Anqi, P. Yulong, S. Guang, Y. Gang, Functions of N6-methyladenosine and its role in cancer, Mol. Cancer 18 (1) (2019) 176.
[10] Y. Wang, J. Wei, L. Feng, O. Li, L. Huang, S. Zhou, et al., Aberrant m5C hypermethylation mediates intrinsic resistance to gefitinib through NSUN2/YBX1/QSOX1 axis in EGFR-mutant non-small-cell lung cancer, Mol. Cancer 22 (1) (2023) 81.
[11] J. Wang, W. Zhu, J. Han, X. Yang, R. Zhou, H. Lu, et al., The role of the HIF-1α/ALYREF/PKM2 axis in glycolysis and tumorigenesis of bladder cancer, Cancer Commun. 41 (7) (2021) 560–575.
[12] I. Barbieri, T. Kouzarides, Role of RNA modifications in cancer, Nat. Rev. Cancer 20 (6) (2020) 303–322.
[13] E. Du, J. Li, F. Sheng, S. Li, J. Zhu, Y. Xu, et al., A pan-cancer analysis reveals genetic alterations, molecular mechanisms, and clinical relevance of m C regulators, Clin. Transl. Med. 10 (5) (2020) e180.
[14] X. Chen, A. Li, B. Sun, Y. Yang, Y. Han, X. Yuan, et al., 5-methylcytosine promotes pathogenesis of bladder cancer through stabilizing mRNAs, Nat. Cell Biol. 21 (8) (2019) 978–990.
[15] Y. Wang, J. Wang, X. Li, X. Xiong, J. Wang, Z. Zhou, et al., N-methyladenosine methylation in tRNA drives liver tumourigenesis by regulating cholesterol metabolism, Nat. Commun. 12 (1) (2021) 6314.
[16] Y. Chen, Z. Lu, C. Qi, C. Yu, Y. Li, W. Huan, et al., N-methyladenosine-modified TRAF1 promotes sunitinib resistance by regulating apoptosis and angiogenesis in a METTL14-dependent manner in renal cell carcinoma, Mol. Cancer 21 (1) (2022) 111.
[17] C. Zhang, L. Chen, W. Lou, J. Su, J. Huang, A. Liu, et al., Aberrant activation of m6A demethylase FTO renders HIF2α clear cell renal cell carcinoma sensitive to BRD9 inhibitors, Sci. Transl. Med. 13 (613) (2021) eabf6045.
[18] W. Li, K. Ye, X. Li, X. Liu, M. Peng, F. Chen, et al., YTHDC1 is downregulated by the YY1/HDAC2 complex and controls the sensitivity of ccRCC to sunitinib by targeting the ANXA1-MAPK pathway, J. Exp. Clin. Cancer Res. 41 (1) (2022) 250.
[19] J. Wu, C. Hou, Y. Wang, Z. Wang, P. Li, Z. Wang, Comprehensive analysis of mC RNA methylation regulator genes in clear cell renal cell carcinoma, Int J Genomics 2021 (2021) 3803724.
[20] Z. Zhang, C. Cao, C. Zhou, X. Li, C. Miao, L. Shen, et al., Identification of a novel 5-methylcytosine-related signature for prognostic prediction of kidney renal papillary cell carcinoma and a Putative target for drug repurposing, Transl Oncol 36 (2023) 101741.
[21] J. Li, X. Liu, Y. Qi, Y. Liu, E. Du, Z. Zhang, A risk signature based on necroptotic-process-related genes predicts prognosis and immune therapy response in kidney cell carcinoma, Front. Immunol. 13 (2022) 922929.
[22] B.T. Lee, G.P. Barber, A. Benet-Pagès, et al., The UCSC Genome Browser database: 2022 update, Nucleic Acids Res. 50 (D1) (2022) D1115–D1122.
[23] Y. Sato, T. Yoshizato, Y. Shiraishi, S. Maekawa, Y. Okuno, T. Kamura, et al., Integrated molecular analysis of clear-cell renal cell carcinoma, Nat. Genet. 45 (8) (2013) 860–867.
[24] S. Alexandra, N. Tavi, A.F. Samuel, A. Arun, B.N. Jacqueline, D.H. Matthew, et al., Contribution of systemic and somatic factors to clinical response and resistance to PD-L1 blockade in urothelial cancer: an exploratory multi-omic analysis, PLoS Med. 14 (5) (2017) e1002309.
[25] W. Hugo, J.M. Zaretsky, L. Sun, et al., Genomic and transcriptomic features of response to anti-PD-1 therapy in metastatic melanoma, Cell 165 (1) (2016) 35–44.
[26] G. Bindea, B. Mlecnik, M. Tosolini, A. Kirilovsky, M. Waldner, A. Obenauf, et al., Spatiotemporal dynamics of intratumoral immune cells reveal the immune landscape in human cancer, Immunity 39 (4) (2013) 782–795.
[27] J. Fu, K. Li, W. Zhang, C. Wan, J. Zhang, P. Jiang, et al., Large-scale public data reuse to model immunotherapy response and resistance, Genome Med. 12 (1) (2020) 21.
[28] S. Hyuna, F. Jacques, L.S. Rebecca, L. Mathieu, S. Isabelle, J. Ahmedin, et al., Global cancer statistics 2020: GLOBOCAN estimates of incidence and mortality worldwide for 36 cancers in 185 countries, CA Cancer J Clin 71 (3) (2021) 209–249.
[29] M. Young, F. Jackson-Spence, L. Beltran, et al., Renal cell carcinoma, Lancet 404 (10451) (2024) 476–491.
[30] J. Eric, W. Cheryl Lyn, R. W Kimryn, Clear cell renal cell carcinoma ontogeny and mechanisms of lethality, Nat. Rev. Nephrol. 17 (4) (2020) 245–261.
[31] J. Hsieh, M. Purdue, S. Signoretti, C. Swanton, L. Albiges, M. Schmidinger, et al., Renal cell carcinoma, Nat Rev Dis Primers 3 (2017) 17009.
[32] S. Delaunay, M. Helm, M. Frye, RNA modifications in physiology and disease: towards clinical applications, Nat. Rev. Genet. 25 (2) (2024) 104–122.
[33] C. Zhang, M. Yu, A.J. Hepperla, et al., Von Hippel Lindau tumor suppressor controls m6A-dependent gene expression in renal tumorigenesis, J. Clin. Invest. 134 (8) (2024) e175703.
[34] S. Li, Z. Jia, J. Yang, X. Ning, Telomere-related gene risk model for prognosis and drug treatment efficiency prediction in kidney cancer, Front. Immunol. 13 (2022) 975057.
[35] Z. Sun, W. Tao, X. Guo, C. Jing, M. Zhang, Z. Wang, et al., Construction of a lactate-related prognostic signature for predicting prognosis, tumor microenvironment, and immune response in kidney renal clear cell carcinoma, Front. Immunol. 13 (2022) 818984.
[36] X. Pan, B. Huang, Q. Ma, J. Ren, Y. Liu, C. Wang, et al., Circular RNA circ-TNPO3 inhibits clear cell renal cell carcinoma metastasis by binding to IGF2BP2 and destabilizing SERPINH1 mRNA, Clin. Transl. Med. 12 (7) (2022) e994.
[37] A. Li, C. Cao, Y. Gan, X. Wang, T. Wu, Q. Zhang, et al., ZNF677 suppresses renal cell carcinoma progression through N6-methyladenosine and transcriptional repression of CDKN3, Clin. Transl. Med. 12 (6) (2022) e906.
[38] L. Li, C. Zhu, S. Xu, Q. Xu, D. Xu, S. Gan, et al., PUS1 is a novel biomarker for evaluating malignancy of human renal cell carcinoma, Aging 15 (11) (2023) 5215–5227.
[39] C. Lang, C. Yin, K. Lin, Y. Li, Q. Yang, Z. Wu, et al., m A modification of lncRNA PCAT6 promotes bone metastasis in prostate cancer through IGF2BP2-mediated IGF1R mRNA stabilization, Clin. Transl. Med. 11 (6) (2021) e426.
[40] A. Latifkar, F. Wang, J. Mullmann, E. Panizza, I. Fernandez, L. Ling, et al., IGF2BP2 promotes cancer progression by degrading the RNA transcript encoding a v-ATPase subunit, Proc Natl Acad Sci U S A 119 (45) (2022) e2200477119.
[41] C. Hu, T. Liu, C. Han, Y. Xuan, D. Jiang, Y. Sun, et al., HPV E6/E7 promotes aerobic glycolysis in cervical cancer by regulating IGF2BP2 to stabilize mA-MYC expression, Int. J. Biol. Sci. 18 (2) (2022) 507–521.
[42] H. Liao, A. Gaur, H. McConie, A. Shekar, K. Wang, J. Chang, et al., Human NOP2/NSUN1 regulates ribosome biogenesis through non-catalytic complex formation with box C/D snoRNPs, Nucleic Acids Res. 50 (18) (2022) 10695–10716.
[43] J. Bi, Y. Huang, Y. Liu, Effect of NOP2 knockdown on colon cancer cell proliferation, migration, and invasion, Transl. Cancer Res. 8 (6) (2019) 2274–2283.
[44] P. McGrath, D. Holley, L. Hamby, D. Powell, C. Mattingly, J. Freeman, Proliferation-associated nucleolar antigen P120: a prognostic marker in node-negative breast cancer, Surgery 116 (4) (1994) 616–620. ; discussion 620-611.

[45] A. Fonagy, C. Swiderski, J. Freeman, Altered transcription control is responsible for the increased level of proliferation-associated P120 in rapidly growing breast carcinoma, Int. J. Cancer 60 (3) (1995) 407–412.
[46] D. Trerè, M. Migaldi, L. Montanaro, A. Pession, M. Derenzini, p120 expression provides a reliable indication of the rapidity of cell duplication in cancer cells independently of tumour origin, J. Pathol. 192 (2) (2000) 216–220.
[47] J. Li, Z. Kong, Y. Qi, et al., Single-cell and bulk RNA-sequence identified fibroblasts signature and CD8 + T-cell - fibroblast subtype predicting prognosis and immune therapeutic response of bladder cancer, based on machine learning: bioinformatics multi-omics study, Int. J. Surg. 110 (8) (2024) 4911–4931.
[48] J. Shi, T. Liu, C. Liu, et al., Remnant cholesterol is an effective biomarker for predicting survival in patients with breast cancer, Nutr. J. 23 (1) (2024) 45.
[49] L. Yao, Y. Shi, J. Fu, et al., Risk factors for invasive pulmonary aspergillosis in patients with severe fever with thrombocytopenia syndrome: a multicenter retrospective study, J. Med. Virol. 96 (5) (2024) e29647.
[50] J. Stenström, I. Hedenfalk, C. Hagerling, Regulatory T lymphocyte infiltration in metastatic breast cancer-an independent prognostic factor that changes with tumor progression, Breast Cancer Res. 23 (1) (2021) 27.
[51] H. Tao, Y. Mimura, K. Aoe, S. Kobayashi, H. Yamamoto, E. Matsuda, et al., Prognostic potential of FOXP3 expression in non-small cell lung cancer cells combined with tumor-infiltrating regulatory T cells, Lung cancer 75 (1) (2012) 95–101.
[52] T. Curiel, G. Coukos, L. Zou, X. Alvarez, P. Cheng, P. Mottram, et al., Specific recruitment of regulatory T cells in ovarian carcinoma fosters immune privilege and predicts reduced survival, Nat Med 10 (9) (2004) 942–949.
[53] A. Sasaki, F. Tanaka, K. Mimori, H. Inoue, S. Kai, K. Shibata, et al., Prognostic value of tumor-infiltrating FOXP3+ regulatory T cells in patients with hepatocellular carcinoma, Eur. J. Surg. Oncol. 34 (2) (2008) 173–179.
[54] Y. Wang, H. Ge, M. Hu, C. Pan, M. Ye, D. Yadav, et al., Histological tumor micronecrosis in resected specimens after R0 hepatectomy for hepatocellular carcinomas is a factor in determining adjuvant TACE: a retrospective propensity score-matched study, Int. J. Surg. 105 (2022) 106852.
[55] H. Zhang, J. Chen, J. Bai, J. Zhang, S. Huang, L. Zeng, et al., Single dual-specific anti-PD-L1/TGF-β antibody synergizes with chemotherapy as neoadjuvant treatment for pancreatic ductal adenocarcinoma: a preclinical experimental study, Int. J. Surg. 110 (5) (2024) 2679–2691.
[56] J. González-Navajas, D. Fan, S. Yang, F. Yang, B. Lozano-Ruiz, L. Shen, et al., The impact of Tregs on the anticancer immunity and the efficacy of immune checkpoint inhibitor therapies, Front. Immunol. 12 (2021) 625783.
[57] T. Atsushi, S. Shimon, Regulatory T cells in cancer immunotherapy, Cell Res. 27 (1) (2016) 109–118.
[58] Y. Shanshan, Z. Yaguang, S. Bing, The function and potential drug targets of tumour-associated Tregs for cancer immunotherapy, Sci. China Life Sci. 62 (2) (2019) 179–186.